Ethylene decomposition on Ir(111): Initial path to graphene formation: Supporting Information

Holly Tetlow, [*] Joel Posthuma de Boer, [‡] Ian J. Ford, [a] Dimitri D. Vvedensky, [‡] Davide Curcio, [b] Luca Omiciuolo, [b] Silvano Lizzit, [c] Alessandro Baraldi, [bcd] and Lev Kantorovich[*]

[*]*Physics Department, King's College London, London, WC2R 2LS, United Kingdom.*

[‡]*The Blackett Laboratory, Imperial College London, London SW7 2AZ, United Kingdom.*

[a]*Department of Physics and Astronomy and London Centre for Nanotechnology, University College London, Gower Street, London WC1E 6BT, United Kingdom.*

[b]*Physics Department, University of Trieste, Via Valerio 2, 34127 Trieste, Italy.* [c]*Elettra – Sincrotrone Trieste S.C.p.A., AREA Science Park, S.S. 14 km 163.5, 34149 Trieste, Italy*

[d]*OM-CNR, Laboratorio TASC, AREA Science Park, S.S. 14 km 163.5, 34149 Trieste, Italy.*

Lowest energy hydrocarbon geometries

For the NEB energy barrier calculations we consider only the lowest energy geometries for the hydrocarbon species. In order to ensure that we find the minimum energy structure for each species we start from many different trial structures and then optimise their geometry. For some species we find multiple geometries and select the one with the lowest binding energy. An example of this is shown for CH_3CH in Figure 1.

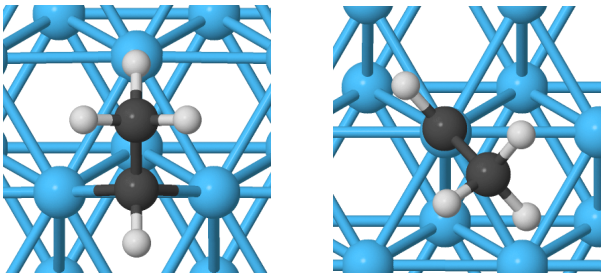

(a) -1.23 eV (b) -0.99 eV

Figure 1: The two geometries found for CH_3CH. The binding energy for the geometry in (a) is 0.24 eV lower than in (b) and is taken to be the default geometry for CH_3CH in all other calculations.

Energy barriers

The energy barriers that we calculate for the various reactions are heavily dependent on the exact choice for the geometries for the initial and final state. For example for a dehydrogenation reaction the position of the hydrogen atom in the final (dehydrogenated) state with respect to its position in the initial intact molecule can affect the energy of the saddle point even though the final state geometries are effectively the same. For this reason we have to be particularly careful when choosing the geometries and ensure that the lowest energy pathway for a reaction is found. For some reactions we have tested different arrangements of the molecule plus an H atom in either the initial or final state in order to find the lowest possible energy barrier for that reaction. This is illustrated in Figure 2 for reaction 13, CHCH $\rightarrow$ CHC + H.

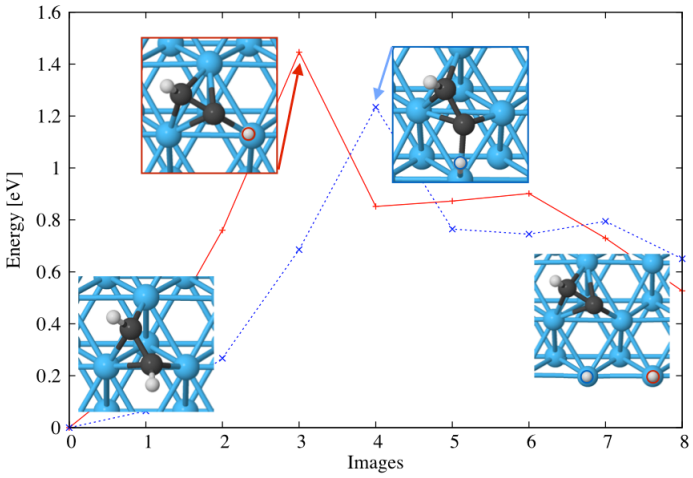

Figure 2: Reaction 13 in detail. The choice of position of the H atom in the final state CHC + H, alters the pathway including the transition state. This changes the energy barrier for the reaction. When placing the H atom in the position marked in blue the energy barrier is 0.22 eV lower than when the position marked in red is used.

Below we show the energy profiles and the initial, final and transition states for all reactions. In each case the configurations are given which have the lowest energy barrier.

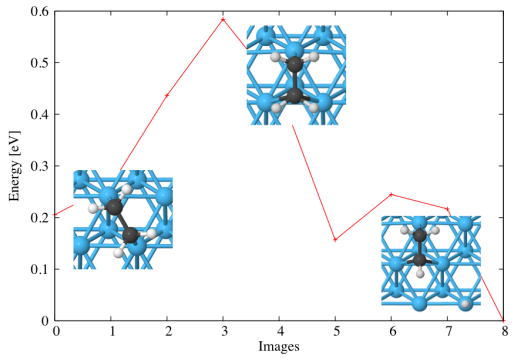

Reaction 1: $CH_2CH_2 \rightarrow CH_2CH + H$

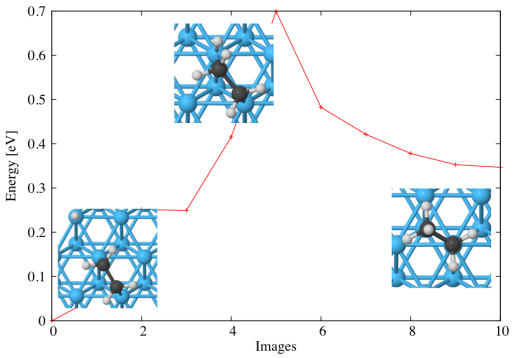

Reaction 2: $CH_2CH_2 + H \rightarrow CH_3CH_2$

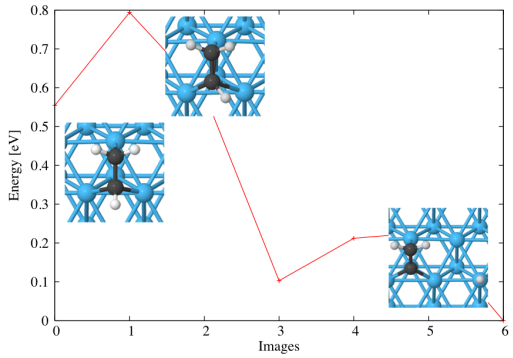

Reaction 3: $CH_2CH \rightarrow CH_2C + H$

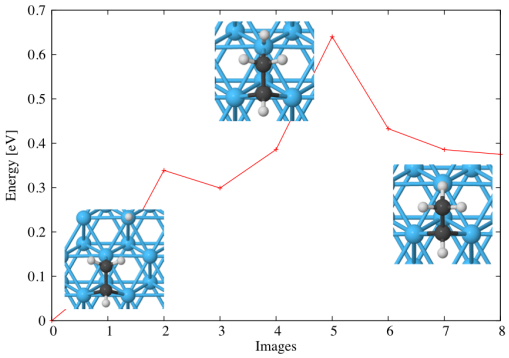

Reaction 4: $CH_2CH + H \rightarrow CH_3CH$

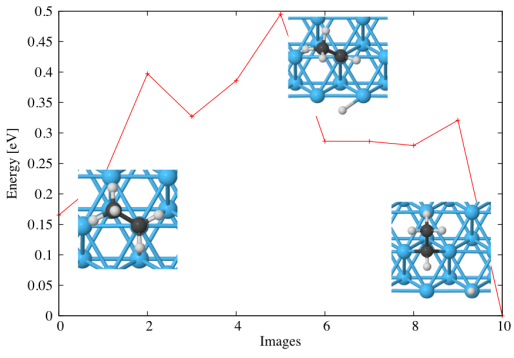

Reaction 5: $CH_3CH_2 \rightarrow CH_3CH + H$

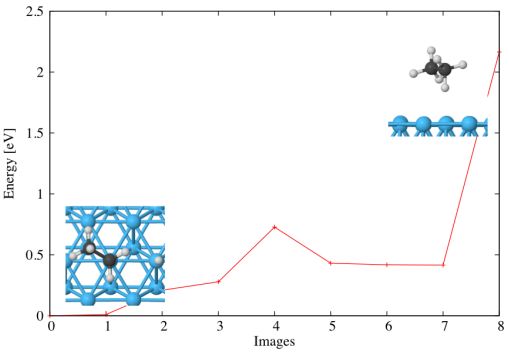

Reaction 6: $CH_3CH_2 + H \rightarrow CH_3CH_3$

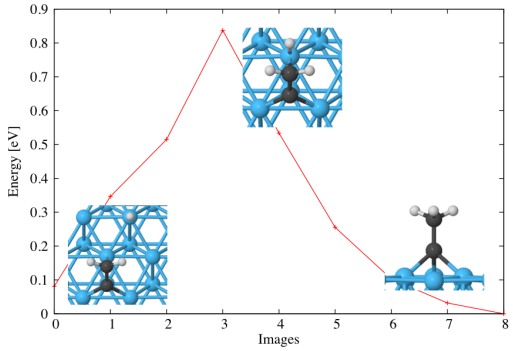

Reaction 7: $CH_2C + H \rightarrow CH_3C$

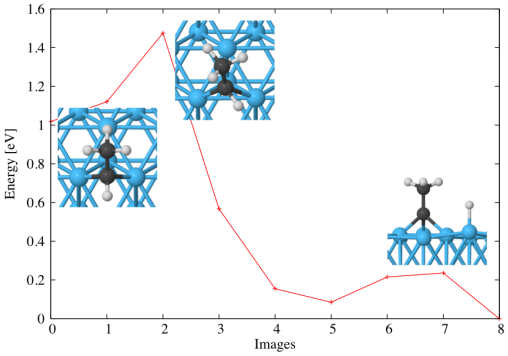

Reaction 8: $CH_3CH \rightarrow CH_3C + H$

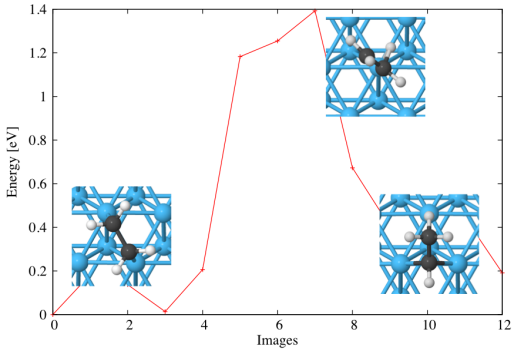

Reaction 9: $CH_2CH_2 \rightarrow CH_3CH$

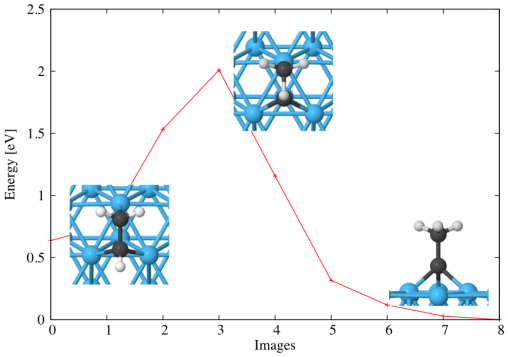

Reaction 10: $CH_2CH \rightarrow CH_3C$

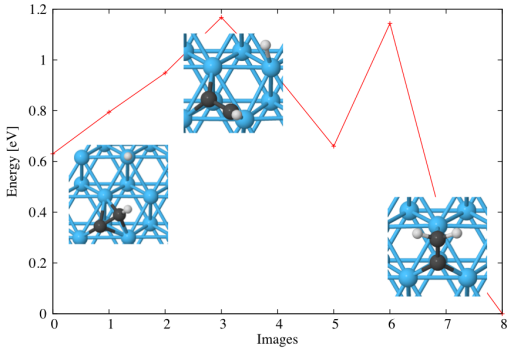

Reaction 11: $CHC + H \rightarrow CH_2C$

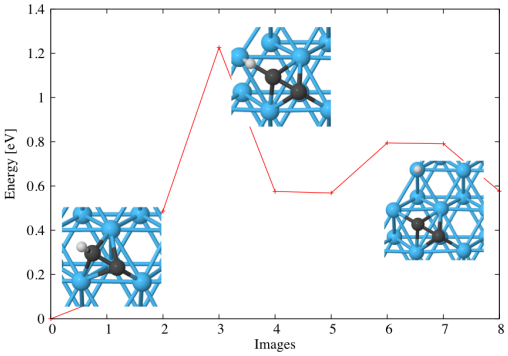

Reaction 12: $CHC \rightarrow CC + H$

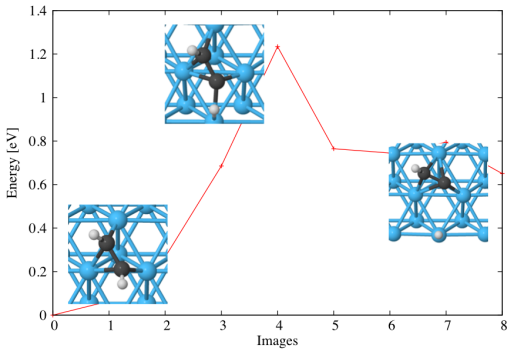

Reaction 13: CHCH → CHC + H

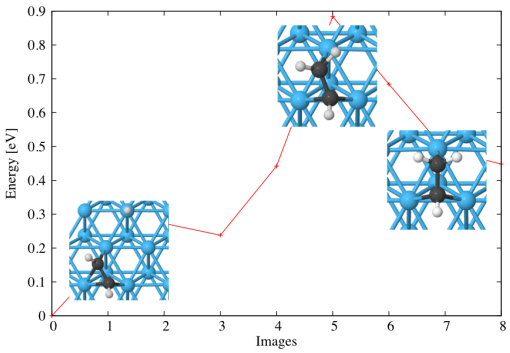

Reaction 14: CHCH +H → CH_2CH

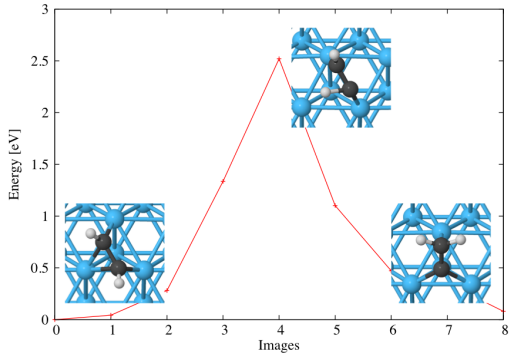

Reaction 15: CHCH → CH_2C

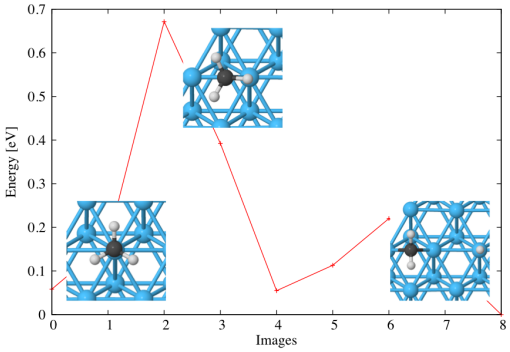

Reaction 16: CH_3 → CH_2 + H

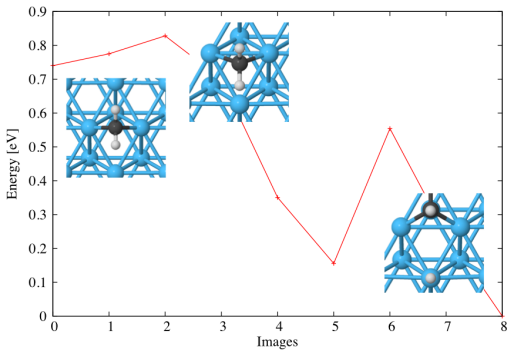

Reaction 17: CH_2 → CH + H

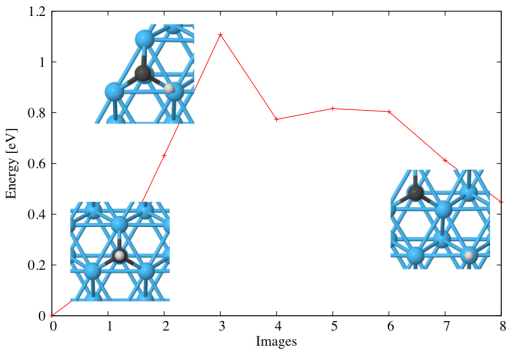

Reaction 18: CH → C + H

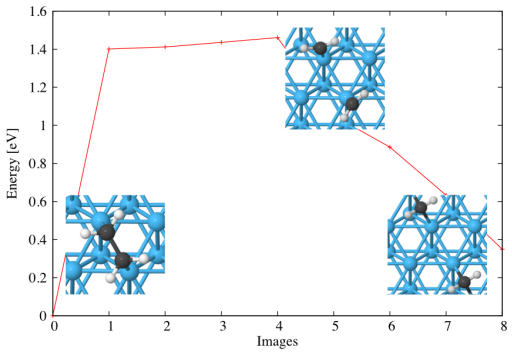

Reaction CB1: $CH_2CH_2 \rightarrow CH_2 + CH_2$

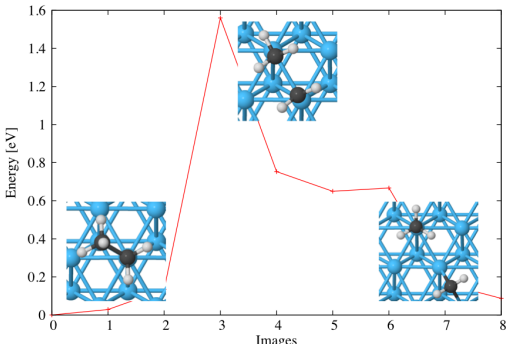

Reaction CB2: $CH_3CH_2 \rightarrow CH_3 + CH_2$

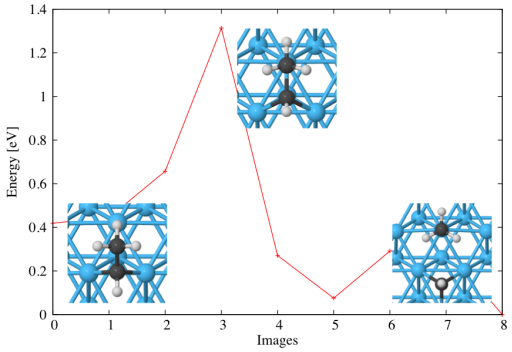

Reaction CB3: $CH_3CH \rightarrow CH_3 + CH$

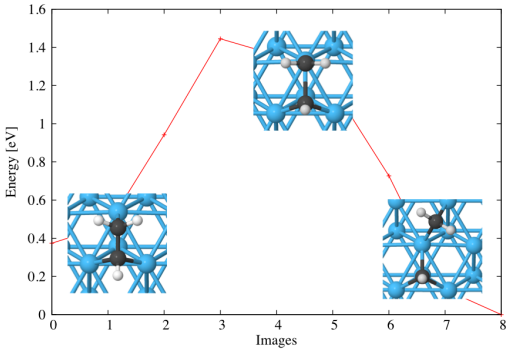

Reaction CB4: $CH_2CH \rightarrow CH_2 + CH$

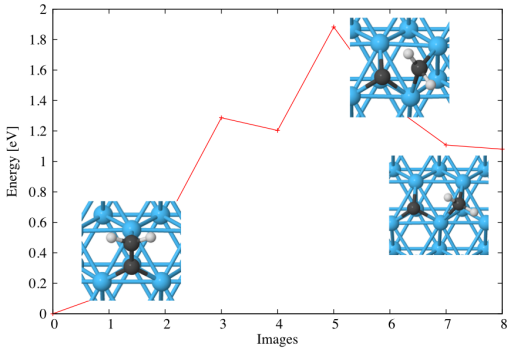

Reaction CB5: $CH_2C \rightarrow CH_2 + C$

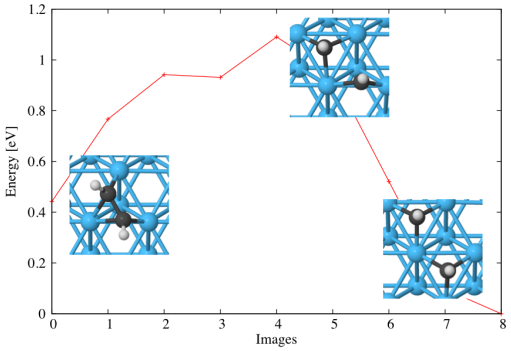

Reaction CB6: $CHCH \rightarrow CH + CH$

Reaction	E_{for} 2L	3L	4L	5L	6L	7L	E_{back} 2L	3L	4L	5L	6L	7L
3	0.24	0.34	0.38	0.35	–	–	0.79	0.65	0.59	0.66	–	–
7	0.76	0.91	0.76	0.84	0.82	–	0.84	0.99	1.01	0.99	0.99	–
14	0.88	0.80	0.71	0.80	0.77	–	0.44	0.55	0.52	0.53	0.53	–
CB6	0.65	1.04	0.82	0.87	0.93	0.79	1.09	1.22	1.15	1.15	1.15	1.13

Table 1: The energy barriers (in eV) for the most important reactions when different numbers of Ir layers are used.

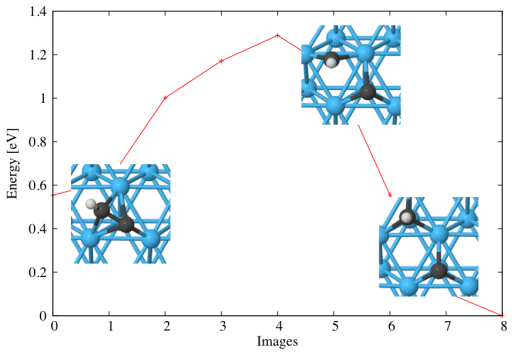

Reaction CB7: CHC → CH + C

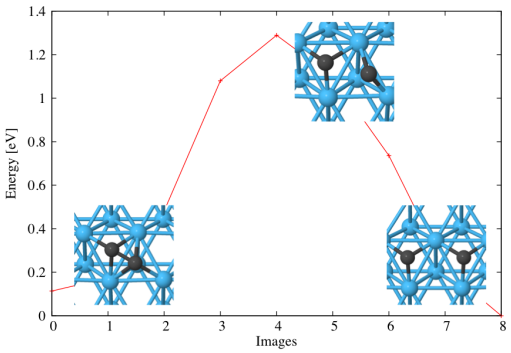

Reaction CB8: CC → C + C

Convergence of energy barriers with number of layers

For the NEB calculations for the energy barriers 2 Ir layers are used for most of the reactions. However we find that the number of layers may affect the value of the barrier by up to 0.2 eV. For the reactions which are not part of the main reaction pathway, or those with significantly large barriers this difference is not enough to greatly affect the final reaction sequence. However for those which are important to the reaction pathway this energy difference can affect the coverages of the various species along the path, especially where two or more barriers have a similar value. Therefore to get an accurate barrier value for these important reactions we sequently add layers to the surface slab used in the NEB calculations and then monitor the convergence. The results are shown in Table 1. For all the reactions apart from reaction CB6 the barriers can be considered as reasonably well converged with less than 6 layers and the result with the most number of layers can be used for the kMC simulations. For the CB6 forward reaction however the converged energy barrier is most likely somewhere between 0.79 and 0.93 eV. Performing additional calculations with even more Ir layers is extremely computationally demanding. Therefore, we decided in this case to run kMC simulations with different values of the barrier within this energy range to determine the effect it has on the coverages and compare with the experimental results. The results of these simulations are shown in Figure 3 for energy barriers of 0.79, 0.85 and 0.93 eV.

When increasing the barrier for the CB6 reaction (CHCH → CH + CH) from 0.79 to 0.93 eV we find that the lifetime of CHCH is increased by about 40 K. This is desirable since the experimental results predict a long lifetime for CHCH. However excessively increasing the barrier results in the formation of

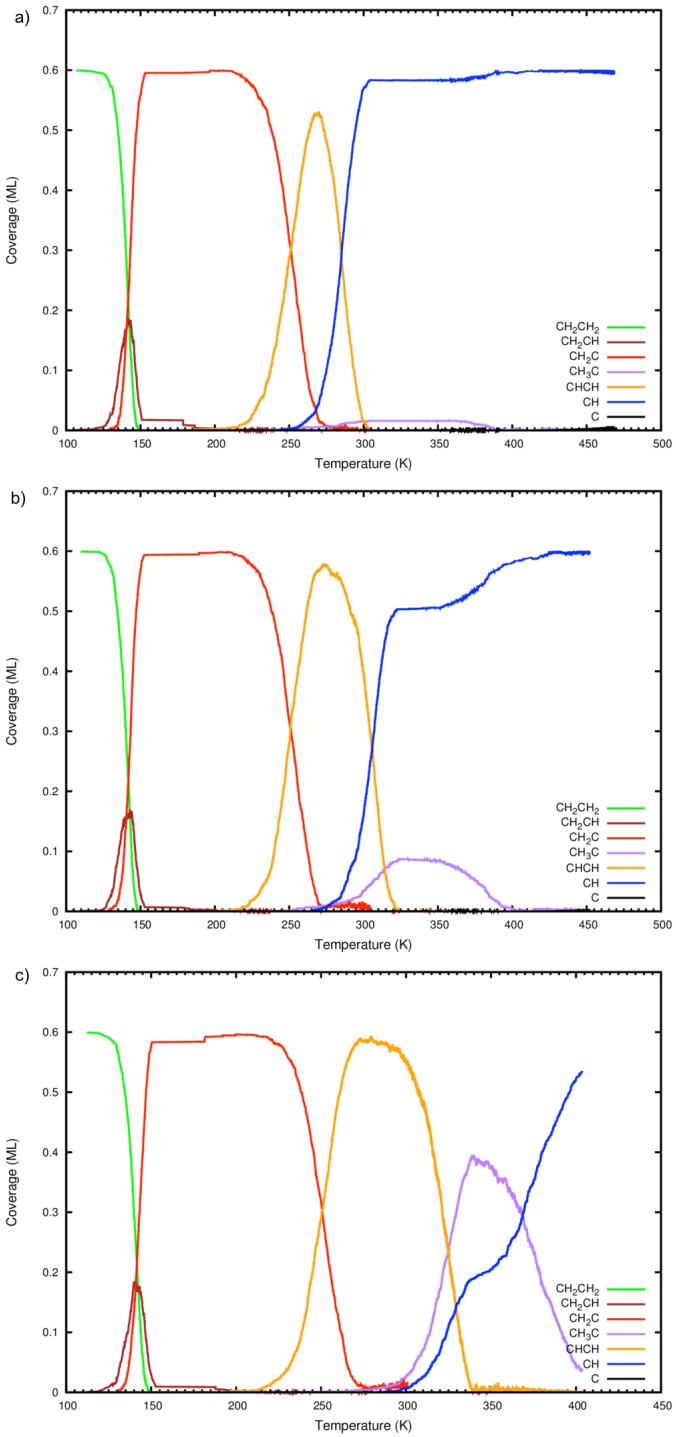

Figure 3: Temperature evolution of species coverage determined from a kMC simulations where the energy barrier for the forward reaction of CB6 are a) 0.79 eV, b) 0.85 eV, c) 0.93 eV.

CH_3C. This is because it is possible to form CH_3C before CHCH can convert into CH.

Lateral interactions

The core level binding energy and NEB calculations assume the case of a low surface coverage. At high coverages the BEs and energy barriers will become altered due to lateral interactions between neighbouring species on the surface. Therefore the values calculated for both the BEs and energy barriers may be different to those in the high coverage experiments. To quantify the changes in the BEs and the energy barriers we performed a single calculation for each with an additional H atom closely neighbouring the hydrocarbon species. This is shown in Figure 4 for CH_2CH ~~(a)~~ and reaction 3 ~~(a) and (b)~~. Since H atoms are produced in abundance for dehydrogenation of ethylene this should be prominent on the surface.

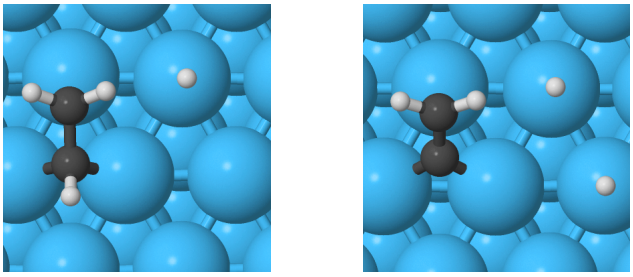

(a) Initial state (CH_2CH) (b) Final state

Figure 4: The (a) initial (CH_2CH) and (b) final states of the modified reaction 3, with ~~a~~ an extra H atom placed nearby in order to see the effect of an neighbouring species on the energy barriers and the core level shift of CH_2CH in (a).

For the CH_2CH molecule + H (shown in Figure 4 (a)) the binding energy associated with the C atom nearest to the H atom was found to change by 0.04 eV due to the presence of the H atom. For the other C atom there was no change in the binding energy. In the case of the NEB calculation E_f was increased by 0.05 eV (17%) and E_b was decreased by 0.03 eV (5%). This is a large enough variation to explain the differences we find between the experimental and theoretical results for the thermal evolution of species.

Pre-exponential factors

Calculating the reaction rates from the energy barriers involves the use of a pre-exponential factor ν, which represents the attempt frequency for the reaction. For this value it is reasonable to take 10^{13} s^{-1}, the atomic vibrational frequency. However for a few key reactions which are important for the reaction mechanism we determine the value of the pre-exponential factors in the equation for their rates. This is done by calculating the vibrational frequencies in the initial, final and transition states and using Vineyard's formula.

As with the energy barriers we also check for convergence with the number of Ir layers for some reactions. The pre-exponential factors do not affect the rates as much as the energy barriers so even a change by one order of magnitude will not greatly change the coverage results.

Reaction	$\nu_{i,j(for)}$ s^{-1} (2lay)	$\nu_{i,j(for)}$ s^{-1} (3lay)	$\nu_{j,i(back)}$ s^{-1} (2lay)	$\nu_{j,i(back)}$ s^{-1} (3lay)
3	1.7×10^{12}	–	5.3×10^{12}	–
7	1.7×10^{13}	8.9×10^{12}	1.2×10^{12}	1.9×10^{12}
14	2.6×10^{13}	1.6×10^{12}	7.8×10^{12}	3.1×10^{12}
CB6	3.6×10^{12}	–	5.9×10^{11}	–

Table 2: The calculated pre-factors ν for 2 (2lay) and 3 (3lay) layers surface slabs.

Hydrogen diffusion

The calculated barriers for H diffusion between several sites are shown in Table 3. All other diffusion pathways (e.g. between two top sites) can be recovered by combining these elementary jumps. The highest barrier calculated (for H diffusion between the top and fcc sites) was 0.36 eV. For H diffusion in the kMC simulation we use the top → fcc value of 0.34 eV to as the barrier to describe the hopping of H atoms from one top site to another.

Diffusion path	E_{for} [eV]	E_{back} [eV]
$H_{top} \rightarrow H_{bridge}$	0.34	0.02
$H_{top} \rightarrow H_{fcc}$	0.36	0.05
$H_{bridge} \rightarrow H_{fcc}$	$\simeq$0.00	0.02
$H_{bridge} \rightarrow H_{hcp}$	0.03	0.01

Table 3: Energy barriers for H diffusion between adsorption sites on the Ir(111) surface.

kMC code

For the kMC code the grid is built up of interlocking triangular sites with circular sites centred on the points where six neighbouring triangular sites intersect. Each triangular site represents a hollow site in the fcc (111) surface and each circular site represents a top site. The hydrocarbon species each have their own configuration on the grid, which is based on the relaxed DFT geometries in the main text. This is shown in Figure 5. They may occupy multiple sites (shaded) on the surface grid depending on their shape. Different orientations are possible due to their rotational degrees of freedom.

To generate the list of reactions at each kMC step the neighbouring sites of each individual species are inspected first. Based on the occupation of these sites certain reactions may only be possible. E.g., for the hydrogenation reaction of a species C_nH_m to take place an H atom must be present at a particular neighbouring top site associated with the formation of the product species C_nH_{m+1}. As an example, all the reactions CH_2CH_2 can undergo are shown in Figure 6.

Next the routine checks whether the product of the particular reaction is allowed, given the sites it will occupy once the original species has undergone the reaction. These are indicated by the green shaded sites in Figure 6. If allowed, then the reaction can be added to the potential reactions list. The kMC algorithm then chooses the reaction at random depending on its relative rate and calculates the time step.

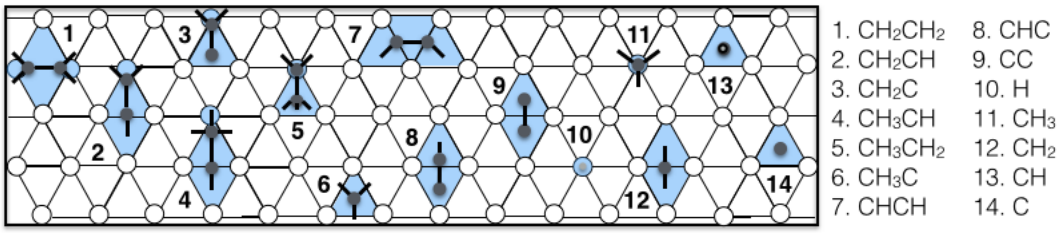

Figure 5: The 14 different species which are included in possible reactions in our kMC simulations. The grid sites shaded in blue show the sites that are considered occupied by each of the species and a cartoon figure of the molecule is overlaid on top. Each species is shown in its 0 degrees orientation (more orientations are accounted for in the simulations).

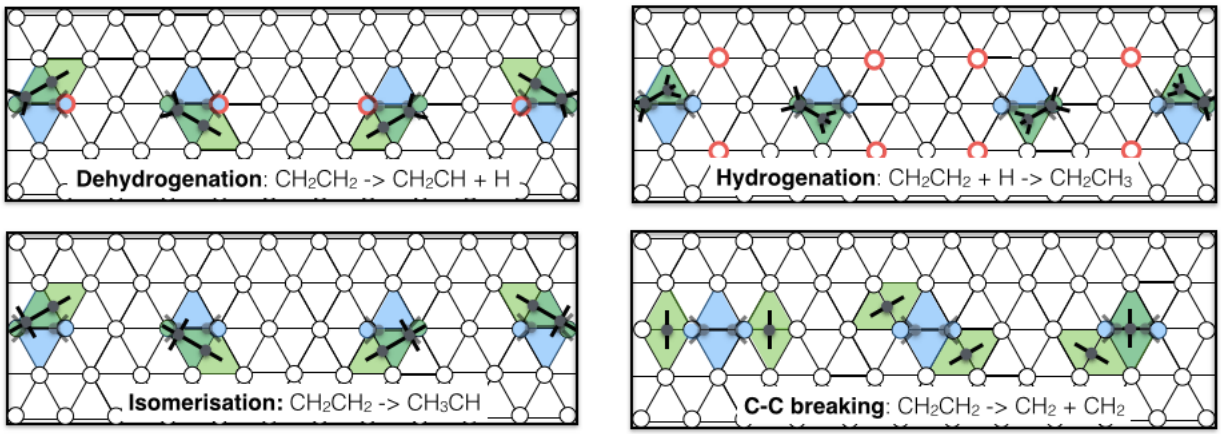

Figure 6: The schematics for the possible reactions with participation of an ethylene molecule: dehydrogenation (top left), hydrogenation (top right), isomerisation (bottom left) and C-C breaking (bottom right). The red circles in the top panels show the positions the removed H atom may occupy in either before hydrogenation or after dehydrogenation reactions. The blue shading shows the sites which are considered to be occupied by ethylene, whereas the green shading shows the sites which are available for the product species to occupy. For simplicity, in each image the ethylene is shown in one of its orientations only. For each reaction the product species can have more than one possible orientation after the reaction (hence there are multiple images for some reactions).

The list of current species and the occupation of the surface sites are updated in accordance with the changes due to the selected reaction.

In our model we include all reactions in listed in the main text. We do not consider the desorption of hydrocarbons and carbon monomers or dimers from the surface; however, the desorption of hydrogen molecules has been included. In this case a desorption reaction is allowed if two H atoms neighbour each other on the grid. Should this reaction be chosen, then both the H atoms are removed directly from the surface grid.

The kMC simulation is initialised with an initial coverage of ethylene molecules which are placed randomly on the surface grid. Based on the sites occupied by an ethylene molecule (two circles and two triangles) we determine that for a 0.6 ML coverage 3/5 of the circular sites should be occupied by ethylene. All other species, including hydrogen, initially have zero concentrations. Over time the temperature is increased linearly as $T = kt + T_0$, where $k = 1.5$ K/s is the experimental rate of increase and $T_0 = 100$ K is the

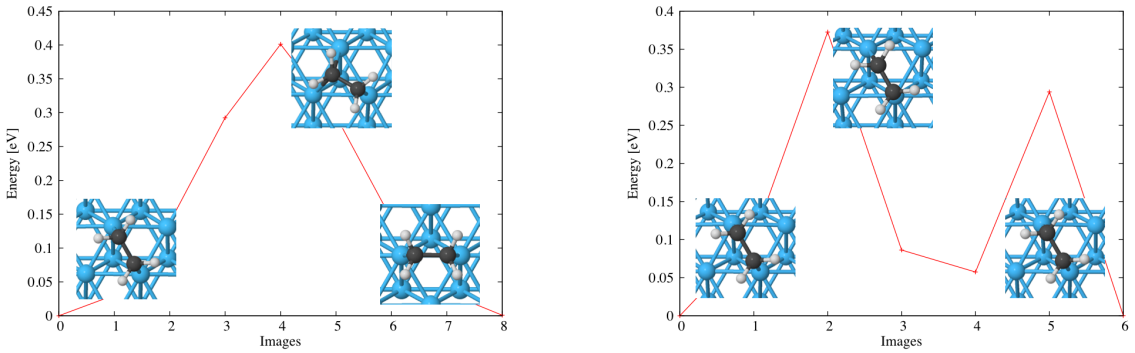

Reaction D1: CH_2CH_2 rotation

Reaction D2: CH_2CH_2 hopping

Figure 7: The energy profiles of the ethylene diffusion mechanisms.

initial temperature of the surface.

Diffusion in kMC

For the kinetic Monte Carlo simulation it is necessary to include the diffusion of the species. To determine the rates of diffusion on the surface for the various species we calculated the diffusion energy barriers. This important to understand whether any of the bimolecular reactions may be limited by the diffusion of the two species to meet each other. Depending on the geometry of a species it may have different diffusion mechanisms, for example ethylene (shown in Figure 7) can diffuse via hopping over a top site or by rotation about a top site. These mechanisms have different energy barriers.

The energy barriers for diffusion of all the hydrocarbon species are below 1 eV. Only the bimolecular reactions (hydrogenation and C-C recombination reactions) are dependent on the diffusion of the two species that need to meet each other before the reaction can happen. If the barriers for the diffusion for both of these species are large compared to the energy barrier for the reaction then we can expect that the reaction will be diffusion limited. However since the barriers for H and the CH_m species diffusion are on average lower than the barriers for the hydrogenation and C-C recombination reactions, respectively, we can expect that these reactions are not diffusion limited. Diffusion does not therefore play the dominant role in the reaction kinetics.

It is possible to consider each diffusion as a separate kMC move in the simulation as with the other reactions. A schematic for the diffusion moves of ethylene is shown in Figure 8. However calculations, in which relatively highly probable diffusion steps are included explicitly, require an extremely large number of kMC steps to be executed, which is prohibitively computationally demanding. Therefore, we applied an acceleration procedure whereby high-rate diffusion steps were effectively executed by randomly rearranging the species on the surface at each step in order to ensure that the surface is homogenised. We have checked this by comparing the results with exact calculation when diffusion moves are included within the kMC algorithm explicitly and found that there is no difference. This work will be the subject of a future paper.

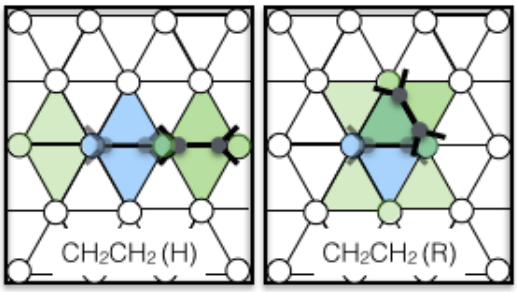

Figure 8: The schematics of ethylene diffusion as used in the kMC code. The blue shading shows the sites which are considered to be occupied by ethylene prior to diffusion, whereas the pale green shading shows the sites that it can diffuse to via each of the mechanisms. For simplicity, in each image the ethylene is shown in only one of its orientations.

Energy barrier tuning

The kMC deduced species coverages show a good qualitative agreement with the experimental results (Figure 6 in the main text). However as previously mentioned, there are noticeable differences in the temperature ranges when certain species appear. Namely the temperature windows for the various species in the kMC results are narrower compared to the experimental results. Due to the inherent error in the DFT calculated energy barriers we believe that the barriers may vary by 5-10% from their calculated values. By adjusting only a few of the energy barriers by this amount it is possible to get a much better agreement with the experimental results. Based on this the energy barrier for reaction 7 can be increased slightly, and the barriers for the reverse reactions 3 and 14 can be decreased, hence suppressing the formation of CH_3C, and promoting the formation of CHCH. The barrier for reaction CB6, which is in the range of 0.79–0.93 eV can be increased from 0.85 to 0.90 eV in order to postpone the CH formation. The changes made to the energy barriers as compared to Table 1 in the main text are shown in Table 4. These changes result in a longer lifetime for CHCH as shown in Figure 9.

	Reaction	E_{calc} [eV]	E_{adjust} [eV]
3_{rev}	$CH_2C + H \rightarrow CH_2CH$	0.66	0.58
7_{for}	$CH_2C + H \rightarrow CH_3C$	0.82	0.85
14_{rev}	$CH_2CH \rightarrow CHCH + H$	0.53	0.48
$CB6_{for}$	$CHCH \rightarrow CH + CH$	0.85	0.90

Table 4: The adjustments made to the energy barriers from the calculated values.

In addition to this we also check the effect of applying a general upward scaling to all barriers. This has the effect of broadening the temperature ranges for each species, which improves the agreement with the experimental results. The thermal evolution of species with energy barriers scaled by +10% are shown in Figure 10. Such scaling may be justified since lateral interactions between species will affect the reaction energetics at high coverages. This would be too complicated to implement properly into the kMC code since there far too many possible reaction scenarios.

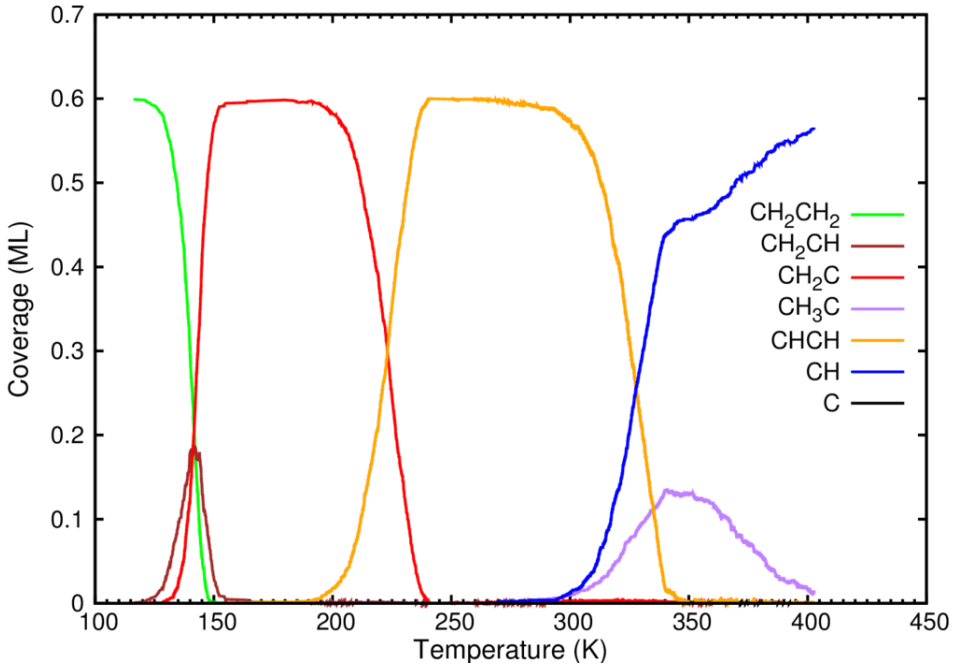

Figure 9: The thermal decomposition of ethylene as determined by kMC when the barriers for particular reactions are adjusted as in Table 4.

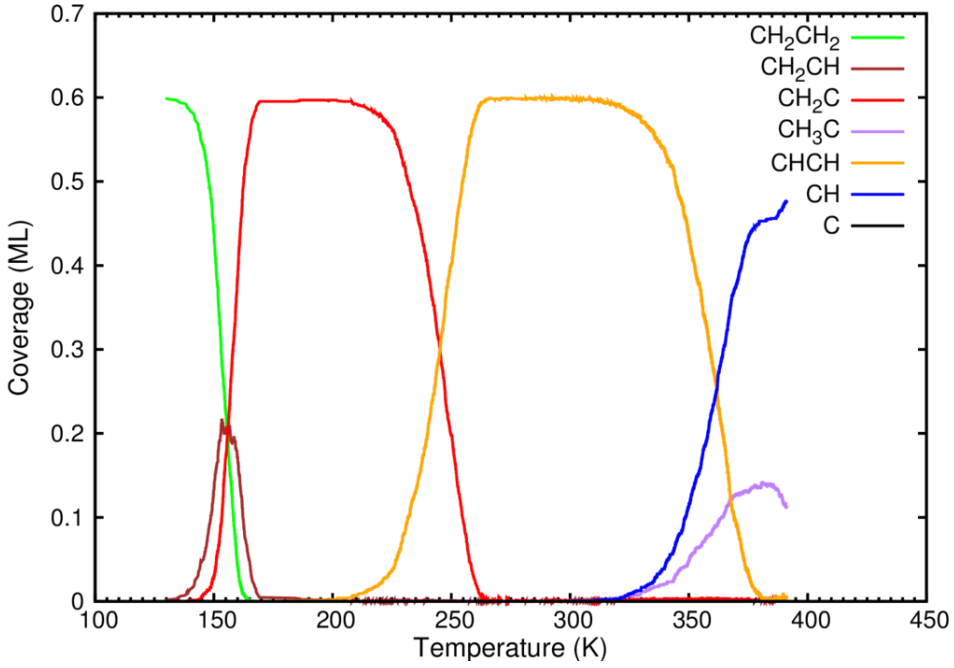

Figure 10: The thermal decomposition of ethylene as determined by kMC when the barriers for particular reactions are adjusted as in Table 4 and scaled by an additional +10% to each barrier.

Vibrational frequency calculations and coverage effects

From observation of Figure 5(a) form the main text it can be seen that there are several peaks differing in their position by about 405 meV. These can be interpreted as belonging to vibrational satellites asso-

ciated with a single species. From the LEED results we also observe at this same temperature range a superstructure due to the adsorbed molecules, representing the c(4×2) structure. To analyse this superstructure and its vibrational satellites we calculated the core level shifts and the vibrational frequencies of the surface modes of the core excited final state for species containing either a single C atom or two equivalent C atoms. Of these species we rule out CH_2CH_2 and CH_2 due to their instability in this temperature range (see energy barriers). Instead we restrict our analysis to the CH-CH, CH and CH_3 molecules. The calculated vibrational frequencies for different coverages are shown in Table 5 for the species with a C core electron shifted to the valence band.

Species	E ($n_c - 1$) [eV]	Vibrational frequencies [meV]
CH-CH	-54.57	(1) 343.0 (2) 378.5
CH	-54.63	341.1
CH_3	-55.49	(1) 340.9 (2) 343.7 (3) 343.9

Table 5: The calculated core level shifts and vibrational frequencies for CH-CH, CH and CH_3 with the c(4×2) superstucture on the Ir surface. For CH-CH the two frequencies correspond to the stretching of the C-H bonds with (1) the core shifted C atom and (2) the regular C atom. For the CH the single frequency is from the stretching of the C-H bond. CH_3 has three frequencies due to (1) the symmetric stretching of all three C-H bonds, (2) the asymmetric stretching of two of the C-H bonds, and (3) two of the C-H bonds stretching in-phase, while the remaining C-H bond stretches out-of-phase.

Out of the three species tested CH-CH has a vibrational frequency closest to the vibrational mode seen in the XPS spectra. For the C atom which is not core shifted the C-H bond gives rise to a vibrational frequency of 381.55 meV for the c(4×4) structure and 378.55 meV for the c(4×2) structure. Compared to the other calculated frequencies that are in the 340-350 meV range this is the most reasonable candidate for the species found experimentally.